# Liquid relative permeability through foam-filled porous media: Experiments

Margaux Ceccaldi, Vincent Langlois, Marielle Guéguen, Daniel Grande, Sébastien Vincent-Bonnieu, Olivier Pitois

# Liquid relative permeability through foam-filled porous media: Experiments

Margaux Ceccaldi[1], Vincent Langlois[1], Marielle Guéguen[2], Daniel Grande[3], Sébastien Vincent-Bonnieu[4], Olivier Pitois[1]

1 Univ Gustave Eiffel, Ecole des Ponts, CNRS, Navier, F-77454 Marne-la-Vallée, France
2 Univ Gustave Eiffel, MAST-CPDM, F-77454 Marne-la-Vallée, France
3 Univ Paris Est Creteil, CNRS, Institut de Chimie et des Matériaux Paris-Est (ICMPE), 2 rue Henri Dunant, 94320 Thiais, France
4 European Space Agency: Keplerlaan 1, 2200 AG Noordwijk, The Netherlands

Abstract:

For some applications involving liquid foams, such as soil remediation for example, the liquid relative permeability of the foam-filled porous medium is a crucial parameter as it sets the liquid flow rate at which active substances or nutrients (for bacteria) can be delivered deep into the medium. We are interested in the liquid relative permeability of foam-filled porous media, within the range of low liquid saturations, i.e. $\lesssim$ 20 vol.%. We fill porous media (packed spherical grains) with different foams made from either alkyl polyglucosides (APG) or saponin, in such a manner that we obtain highly controlled samples in terms of the bubble-to-grain size ratio $r$ and the liquid saturation. The liquid relative permeability of saponin samples exhibits an optimal value as a function of $r$, while it increases significantly for APG foams. The ratio of their relative permeability APG/saponin reveals two regimes as a function of $r$: for $r \lesssim 0.25$, the permeability ratio is equal to the ratio corresponding to the bulk foams, while for larger $r$ values, the permeability ratio is increased by one order of magnitude. The foam microstructure changes a lot as the bubble-to-grain size ratio increases up to 0.5, so that a new liquid network is activated, made of surface channels and liquid bridges, the former connecting the latter even at low liquid saturation. These new liquid elements may greatly benefit foams with mobile interfaces such as APGs. One such issue would deserve a dedicated study to be elucidated.

## I. INTRODUCTION

Liquid foams are used in various applications [1]. In the context of soil remediation [2] or oil extraction [3], foam rheology is useful to mitigate effects due to permeability contrast within the soil layers. In the presence of foam into porous media, it is usual to describe the flows of both gas and liquid phases in terms of relative permeability which can be correlated to the phase saturation using Corey-type relations [4] for example. Such relations involve several parameters, such as the so-called end point relative permeability to the considered phase, the irreducible water saturation and the residual gas saturation, as well as Corey exponents. In a pioneering work, Bernard *et al*. [5] studied the effect of foam on permeability of porous media to water. It was concluded that the presence of foam did not change the liquid (water) relative permeability. In other words, the permeability to liquid was the same in the presence or in the absence of foam lamellae. This result, which is currently used as a basic assumption in models for foams through porous media, has been strengthened recently by Eftekhari & Farajzadeh [6].

Herein, we are interested in the liquid relative permeability of foam-filled porous media within the range of low liquid saturations, *i.e*. 5%-20 vol.%, whereas most of the previous studies were performed at significantly higher liquid saturations, *i.e.* > 20 vol.%. Our goal is to demonstrate that there are situations where the characteristics of the foam trapped into the porosity has significant impact on liquid permeability. In order to show this, we have to be able to control the bubble-to-grain

size ratio (with both monodisperse bubbles and grains), which is expected to have significant effect: for small ratio the pores are filled with foam, while for ratio close to unity each pore will contain one bubble on average. We also have to be able to control the liquid contained. And, in order to fully address this issue, we will also play with the mobility parameter of the surfactants along the liquid/air interfaces. As such a control has never been carried out in the past we hope to obtain original results.

## II. MATERIALS AND METHODS

### A. Foaming solution

Two foaming solutions were studied.

(1) Saponin (from Merck) was used as a nonionic surfactant. It is extracted from the Quillaja Saponaria barks. Note that the word 'sapo' (Latin) means 'soap', which is due to the fact that saponins form foams when mixed with water. The amphiphilic structure of saponins, due to their lipophilic aglycones and hydrophilic saccharide side chains, is responsible for the foam formation. We used this product as received at concentration 6 g/L in water (milli-Q). It is composed of 8 % to 25 % of sapogenin and its average molar mass is 1000-2000 g/mol. The CMC was measured to be about 3.3 g/L.

(2) Alkyl polyglucosides (Glucopon® 225DK from BASF) used at 10 g/L in water. It is an anionic surfactant of average molar mass 420 g/mol, and its purity is equal to 70 %. The CMC was measured to be about 2 g/L.

### B. Porous medium

The porous medium was made by piling monodisperse grains (glass beads) in a glass column. Grains diameter $D_p \pm \Delta D_p$ ranges from 1.1 mm to 5 mm (see Table 1), with $\Delta D_p/D_p \approx 5\%$ for grains of size 1.5, 3 and 5 mm, $\Delta D_p/D_p \approx 8\%$ for 1.1 mm grains, and $\Delta D_p/D_p \approx 10\%$ for the 2.0 mm grains. The first step is to determine the pore volume that the foam will occupy in the packing. The porosity $\phi_p$ of the grains packing is likely to be influenced by wall effects in the column of diameter 25.9 mm. Specifically, the arrangement of grains at wall is different from the volume packing, and the proportion of pores exposed to the wall varies with the ratio of grain/column diameters, i.e. 0.04 to 0.2. We determine the porosity as follows: a mass of grains $m_g$ is poured into a column partially filled with water with a volume $V_e$. We distinguish two characteristic volumes for the packing: $V_g$ corresponding to the volume of all the grains added (we don't know this volume, but we will determine it in the following) and $V_{pack}$ corresponding to the total volume occupied by the packing. The total volume of water and grains is noted $V_t$. The density is obtained with the ratio: $C_g = m_g/V_g = m_g/(V_t - V_e)$. Thereafter the volume of grains introduced into the column was determined by the ratio $m_g/C_g$. Before filling the column with the grains, their mass is weighed. A grid is added to the bottom of the column so that the grains were retained in the column while allowing the foam to pass without breaking the bubbles. After filling, the height $H$ of the packing is measured and its volume $V_{pack}$ is determined from the cross-section $S$ = 527 mm$^2$ of the column. The porosity is then calculated by the relation $\phi_p = 1 - m_g/(C_g V_{pack})$. $\phi_p$ values are presented in Table 1.

| $D_p$ | 5 mm | 3 mm | 2 mm | 1.5 mm | 1.1 mm |
|---|---|---|---|---|---|
| $\phi_p$ (H = 160 cm) | 0.43 | 0.42 | | | |
| $\phi_p$ (H = 64 cm) | | 0.39 | 0.38 | 0.41 | 0.38 |

*Table 1: Diameter $D_p$ of the grains (glass beads) used to make the packings and the resulting pore volume fraction $\phi_p$. H is the height of the column in which the grains have been packed.*

C. Foam production and filling of the porous medium

We used the device already implemented in previous reports [7–10] and shown in Fig. 1a. The setup and the procedure are briefly presented in Appendix A.

The resulting foam continuously fills the porous column. We monitored the foam at the exit of the column until we found the monodisperse foam introduced. Therefore, at that stage, the size (volume) of the bubbles inside the bead pack is the one we have prepared in the foaming column. It may be necessary to circulate foam for a few minutes before the stability described above is observed. As preliminary tests, after the described non-stationary phase, we measured the liquid fraction of the foam contained into the porous column by comparison of the mass of the foam-filled porous column with the one of the initially dry porous column. All the measurements were found to be within the error bar (*i.e.* 5%) of the liquid fraction measured at the entry of the porous column, which means that the target liquid fraction was reached. Because of gas compressibility, one could expect some deviation with respect to the latter estimation. However, while moderate driving pressure is required to fill the column, after the arrest of the flow, the foam pressure is released through both column's ends, resulting eventually in a remaining pressure originating from the trapping of the bubbles into the pore network. For the studied porous columns, this pressure is expected to be of the order of $P = P_0 + 10^3 Pa$ and the resulting change in foam liquid fraction is given by $\varepsilon_f(P)/\varepsilon_f(P_0) = 1/\left(1 + \left(1 - \varepsilon_f(P_0)\right) P_0/\varepsilon_f(P_0)P\right) \approx 1\%$.

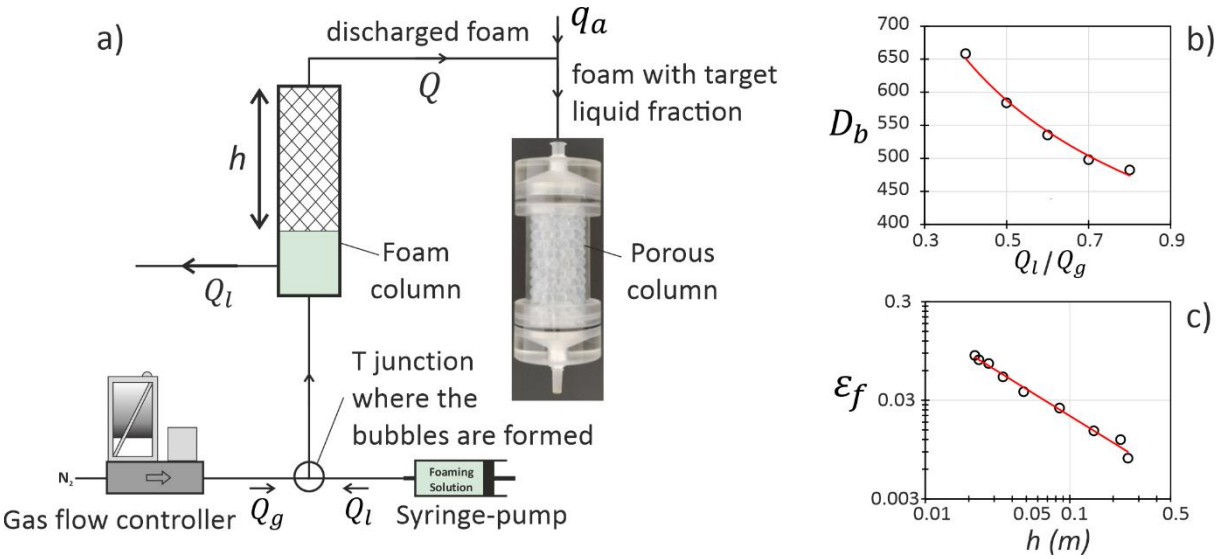


*Figure 1: Setup used to prepare liquid foam and fill the porous media. Both bubble size ($D_b$) and liquid volume fraction ($\varepsilon_f$) of the discharged are set during foam preparation – see (b) and (c) respectively. All the details can be found in the Appendix A.*

D. Permeability measurement

First, we measured the reference permeability $k_{f0}$ of bulk foam alone, i.e. without any effect of confinement by the porous medium. This was done using the method known as *forced drainage* [11,12]. Then, for a few foam-filled porous samples, essentially those with large grains (3 and 5 mm) and APG foams, we extend this method to determine the permeability $k_f$ of the confined foam. For the other foam-filled porous samples, we turned to a falling head permeability test to determine $k_f$. The Appendix B presents all the details for both methods.

## III. Results and Discussion

First, we consider the results for both saponin and APG bulk foams presented in Fig. 2a. As expected, the permeability increases as a function of liquid fraction [13]. Besides, foam made with APG is significantly more permeable than foam made with saponin. Both foam permeabilities are shown to be correctly described over the full range of liquid fraction by expressions proposed in the literature [14], which account for the ability of the surfactant-laden interfaces to be set in motion or to resist to viscous stress from liquid flow between the bubbles. Therefore, the permeability of the saponin foam is well-described by eq. 1a, which corresponds to "non-mobile" interfaces, while the APG foam corresponds to "mobile" interfaces and is well-described by eq. 1b. Note that here, the terms "mobile" and "non-mobile" refer to the tangential mobility of the surfactant along the liquid-gas interface. Therefore, the surfactants chosen for the present study exhibit the extreme interfacial behaviors that can be observed for the drainage of liquid foam [14]. The ratio of the dimensionless permeabilities $\tilde{k}_{f0}^{APG}/\tilde{k}_{f0}^{sap}$ is close to 5 for most of the values, except for liquid fractions $\varepsilon_f < 0.02$.

$$\tilde{k}_{f0}^{sap}(\varepsilon_f) = \frac{k_{f0}^{sap}(\varepsilon_f)}{D_b^2} = \frac{{\varepsilon_f}^2}{\alpha_0\left(1 - 2.15\varepsilon_f + 1.37{\varepsilon_f}^2\right)^2} \quad (1a)$$

$$\tilde{k}_{f0}^{APG}(\varepsilon_f) = \frac{k_{f0}^{APG}(\varepsilon_f)}{D_b^2} = \frac{{\varepsilon_f}^{3/2}}{\beta_0\left(1 - 2.7\varepsilon_f + 2.2{\varepsilon_f}^2\right)^2} \quad (1b)$$

where $\alpha_0$ = 1350 and $\beta_0$ = 1250 were obtained from least square fits of figure 2a. It is noteworthy that in the limit of small liquid fractions, these expressions are compatible with the well-known *Plateau border model*, i.e. $\tilde{k}_{f0} \sim {\varepsilon_f}^2$, and the *vertex model*, i.e. $\tilde{k}_{f0} \sim {\varepsilon_f}^{3/2}$ [13].

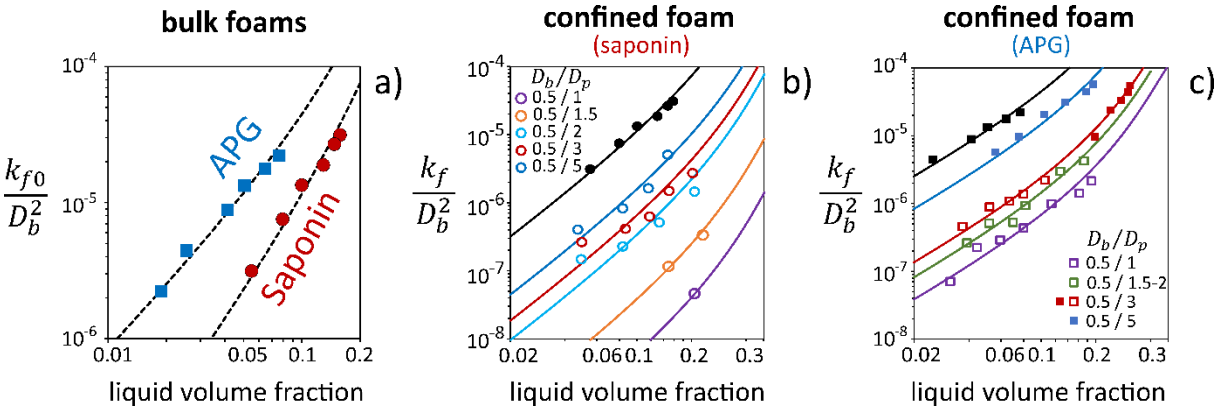

*Figure 2: (a) Reference dimensionless permeability $\tilde{k}_{f0} = k_{f0}/D_b^2$, i.e. the bulk (non-confined) permeability divided by the bubble diameter squared, as a function of the liquid volume fraction for the two foams used in this study, namely Saponin foam and APG foams. Dotted lines correspond to equations 1a and 1b. (b) Dimensionless permeability $\tilde{k}_f = k_f/D_b^2$ measured as a function of liquid volume fraction (i.e. $\varepsilon_f$ or equivalently the liquid saturation $S_w$) for the confined saponin foams, for different bubble/grain sizes, as indicated (in mm). Black symbols correspond to the reference foam. Solid lines correspond to eq. 2 with coefficient $C(r)$ presented in Figure 4a. (c) Dimensionless permeability $\tilde{k}_f = k_f/D_b^2$ measured as a function of liquid volume fraction (i.e. $\varepsilon_f$ or equivalently the liquid saturation $S_w$) for the confined APG foams, for different bubble/grain sizes, as indicated (in mm). Black symbols correspond to the reference foam. Solid lines correspond to eq. 2 with coefficient $C(r)$ presented in Figure 4a.*

Then, we present the results of the foam confined into the porosity of granular packings. In Figs 2b and 2c, foam permeabilities $\tilde{k}_f$ of confined foams with same bubble size, *i.e.* $D_b$= 500 µm, are plotted as a function of liquid fraction for different grain diameters $D_p$, for saponin and APG respectively. Both $\tilde{k}_f^{sap}$ and $\tilde{k}_f^{APG}$ show significant decrease with respect to the corresponding $\tilde{k}_{f0}$ value as $D_p$ decreases from 5 mm to 1 mm. Actually, $\tilde{k}_f^{sap}$ is decreased by about 1000 and $\tilde{k}_f^{APG}$ is decreased by about 100. For APG foams, measurements performed with both the 'front' method and the Darcy method are found to be complementary and fit together to form a consistent curve (see Fig. 2c for $D_p$ = 3 mm and 5 mm). As seen in Fig. 2c, data for $D_p$ = 1-1.5 mm were scarce because it was difficult to ensure the foam stability with saponin during the filling step for such grain sizes.

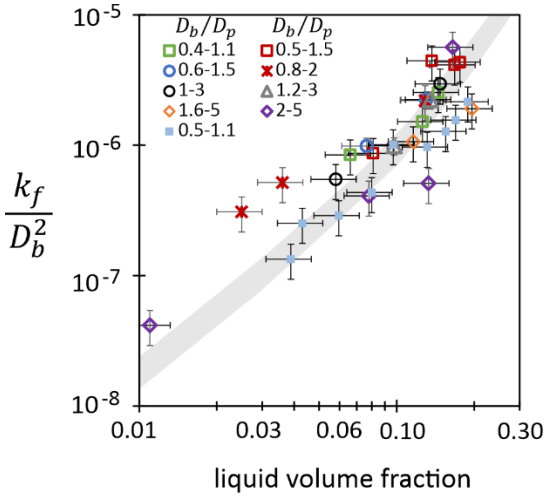


*Figure 3: Dimensionless permeability $\tilde{k}_f = k_f/D_b^2$ measured as a function of liquid volume fraction (i.e. $\varepsilon_f$ or equivalently the liquid saturation $S_w$) for confined APG foams, for different bubble/grain sizes, as indicated (in mm). All the presented size ratios are within the range $0.32 \leq r \leq 0.46$. The thick grey line frames to values obtained from equation 2 with $C(r = 0.32) = 0.029$ and $C(r = 0.46) = 0.0175$. As a reasonable collapse is obtained, this suggests that $r$ and liquid fraction can be considered as control parameters.*

In order to investigate the respective effects of both grain diameter $D_p$ and bubble diameter $D_b$, we present in Fig. 3 different combinations of those parameters leading to $r = D_b/D_p$ values within a narrow range $0.32 \leq r \leq 0.46$. Fig. 3 shows that the relevant control parameter for the dimensionless permeability of confined foams is actually the size ratio $r$: whatever the grain size, the dimensionless

permeability $k_f(\varepsilon_f)/D_b^2$ of the confined foam is set by $r$. More precisely, $k_f$ can be deduced from $k_{f0}$ by the following relation:

$$\tilde{k}_f(r,\varepsilon_f) = C(r) \times \tilde{k}_{f0}(\varepsilon_f) \qquad (2)$$

where the values of $C(r)$ that permit to describe the curves $\tilde{k}_f(r,\varepsilon_f)$ in Figs 2b and 2c are presented in Fig. 5a. It is noteworthy that we were able to fit our data by keeping the form of equations 1 and changing only the coefficients $\alpha_0$ and $\beta_0$ which we replaced with $\alpha(r)$ and $\beta(r)$ respectively. Therefore, coefficients $C(r)$ are the ratios $\alpha(r)/\alpha_0$ and $\beta(r)/\beta_0$ respectively. As expected we find for $C(r)$ the decrease already observed in Figs 2b and 2c. It is to say that the strong decrease for saponin foam is almost an exponential decrease. For APG foam the decrease is similar at small $r$ values, i.e. $r \leq 0.25$, while the decay is more limited at larger $r$ values. It is usual to express the permeability of the foamy porous medium $k_D$ in terms of relative permeability, i.e. $k_{rel} = k_D/k_D(S_w = 1)$. In order to provide values for $k_D(S_w = 1)$, we choose to use the Carman-Kozeny expression for the permeability of the saturated granular pack[15,16]: $k_{CK} = \phi_p^3 D_p^2 / \left[180(1-\phi_p)^2\right]$. According to eqs (B6) and (2) the relative permeability writes:

$$k_{rel} \equiv \frac{k_D}{k_{CK}} = 180\left(\frac{1-\phi_p}{\phi_p}\right)^2 r^2 C(r) \times \tilde{k}_{f0}(\varepsilon_f) \qquad (3)$$

Therefore, $k_{rel}$ depends on the liquid volume fraction $\varepsilon_f$, also called liquid (water) saturation $s_w$, through $\tilde{k}_{f0}(\varepsilon_f)$, which accounts for the intrinsic permeability of the bulk foam. It is interesting to plot the functional form $r^2C(r)$ which accounts for the effects of confinement by the grains (see Fig. 4b). For saponin foam, the function increases from $r \approx 0$ to $r \approx 0.1$, then decreases for $r \geq 0.25$. As a result, there is a range of values $r$ corresponding to maximum relative permeability for the foamy granular packings. In contrast, for APG foam, there is a monotonic increase. The effect of the surfactant is therefore considerable as it induces either an increase or a decrease of the relative permeability for $r \geq 0.25$, all other parameters being equal. Moreover, the use of APG foam instead of saponin, or more generally: the use of foam exhibiting 'mobiles' interfaces instead of foam exhibiting 'non-mobiles' interfaces, allows to increase significantly the relative permeability of foamy granular packing, all the more so as the bubble-to-grain size ratio $r$ is larger than 0.25. This can be seen also in Fig. 4c where the ratio $k_{rel}^{APG}/k_{rel}^{sap}$ is plotted as a function of $r$ (note that as the data for the two surfactants do not have exactly the same r values, we performed linear interpolations to make them match). Two regimes can be clearly distinguished: (1) for $r \leq 0.25$, the permeability ratio of the confined foams is comparable to the ratio corresponding to the bulk foams, i.e. $k_{rel}^{APG}/k_{rel}^{sap} \approx \tilde{k}_{f0}^{APG}/\tilde{k}_{f0}^{sap} \approx 5$; (2) for $r > 0.25$ the permeability ratio of the confined foams is one order of magnitude larger than the ratio corresponding to the bulk foams, i.e. $k_{rel}^{APG}/k_{rel}^{sap} \gg \tilde{k}_{f0}^{APG}/\tilde{k}_{f0}^{sap}$.

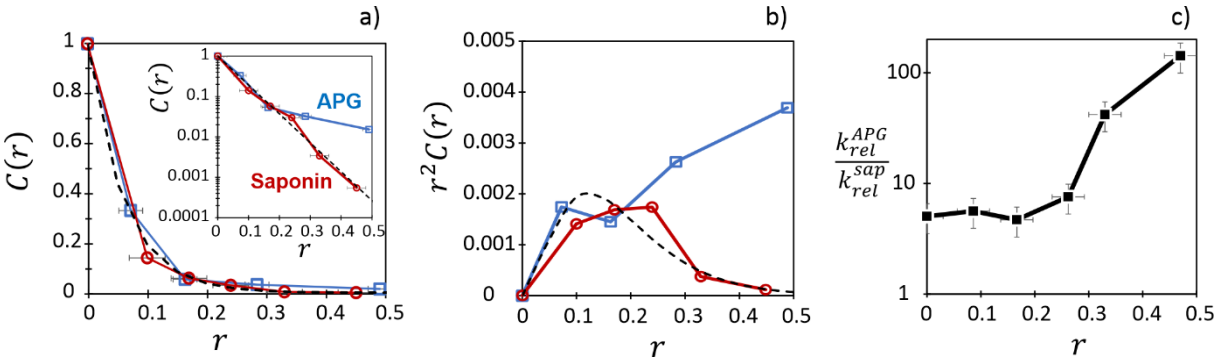

Figure 4: (a) Coefficient $C(r)$ introduced in equation 8 to describe the decrease in the dimensionless permeability as a function of the bubble-to-grain size ratio, with respect to the reference bulk foam (not confined). Inset: Same data but with log-scale for $C(r)$. Dotted lines correspond to $C(r) = exp(-r/0.0607)$. (b) Functional form $r^2C(r)$ which accounts for the effects of confinement by the grains in the expression of the relative permeability, i.e. permeability of the foam-filled porous sample divided by the permeability of the liquid-saturated porous sample (see equation 3). The dotted line corresponds to $r^2C(r) = r^2 \times exp(-r/0.0607)$. (c) Ratio of permeability of APG/saponin foam-filled porous samples as a function of bubble-to-grain size ratio. The point at $r = 0$ is related to the corresponding bulk foams.

It is shown here that the bubble-to-grain size ratio is a crucial parameter for relative permeability within the range of low liquid saturations. It can be said that a stronger foam confinement associated with the increase of the bubble-to-grain size ratio is responsible for this effect. More precisely, the decrease in the density of bulk foam channels to the advantage of surface channels is expected to be directly related to the observed decrease of the liquid permeability. Observations of ours samples at the wall revealed that for high bubble-to-grain size ratio, bulk liquid channels have disappeared, whereas significant liquid proportion is in contact with the grain surface, either wall in the form of wall liquid channels or in the form of liquid bridges, the former connecting the latter even at low liquid saturation (see Figure 5). Because the foam microstructure changes significantly as the bubble-to-grain size ratio increase up to 0.5, one can imagine that a new liquid network is activated and replaces the liquid network specific to bulk foams. This new network may have elements that can greatly benefit foams with mobile interfaces. This issue would deserve a dedicated study to be elucidated.

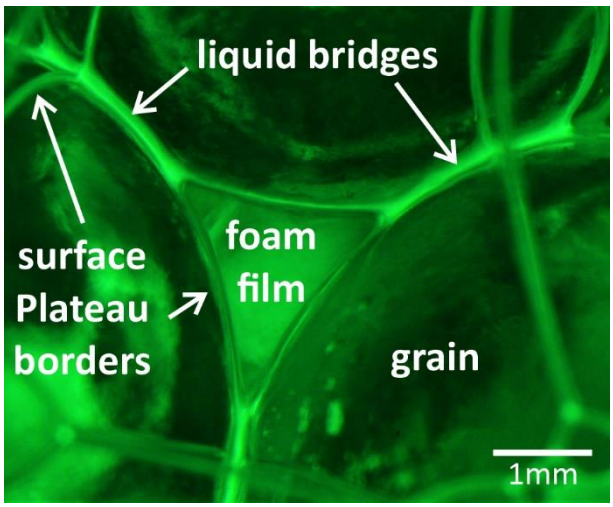


Figure 5: Picture of a sample as observed through the wall, for high bubble-to-grain size ratio (i.e. $r \approx 0.5$). The liquid content has been made very low (i.e. 2-4 vol.%) in order to better see the foam microstructure. The liquid bridges form at contact between adjacent grains, and the surface channels (surface Plateau borders) connect the liquid bridges. Foam films also connect both surface Plateau borders and liquid bridges. This is to say that there are no more bulk pore liquid channels.

## IV. CONCLUSION

We measured liquid permeability values of foam-filled bead packs for low liquid volume fraction (equivalently, low liquid saturation). We were able to control independently the bubble size, the grain

size, the liquid saturation, and the effective mobility of the foam interfaces. With respect to this last parameter, this was achieved by using two different surfactants, namely alkyl polyglucosides (APG), which was shown to exhibit the so-called mobile interfaces [13], and saponin, which was shown to exhibit the so-called non-mobile interfaces [13].

Liquid permeability in foam-filled samples was measured for liquid saturations as low as 3 vol.% for both surfactants. We showed that when using the reference foam (non-confined) permeability, made dimensionless with the bubble size squared, the confined foam permeability decreased as a single function of the bubble-to-size ratio, $r$. This function depended however on the surfactant, and we reported a decrease for saponin stronger than that for APG.

In contrast to the conclusions drawn by Bernard [5] from his pioneering work, and more recently by Eftekhari & Farajzadeh [6], we prove that there are conditions where the foam controls the liquid relative permeability. Expressed in terms of relative permeability of the porous medium, *i.e*. permeability of the foam-filled sample divided by the permeability of the liquid-saturated sample, we observed a strong effect of the used surfactant as a function of the bubble-to-grain size ratio. For saponin, a non-monotonic curve is obtained, exhibiting a maximum value for values of $r$ close to 0.15-0.2. For APG, we measured an increasing function. This difference was also highlighted when plotting the ratio of the relative permeability (APG/saponin): (1) for $r \leq 0.25$, the permeability ratio of the confined foams was approximately equal to 5, which was comparable to the ratio corresponding to the bulk foams; (2) for $r > 0.25$, the permeability ratio of the confined foams is one order of magnitude larger than the ratio corresponding to the bulk foams.

Bernard *et al*. [5] studied the effect of foam on permeability of porous media to water. It was concluded that the presence of foam did not change the liquid (water) relative permeability. In other words, the permeability to liquid was the same in the presence or in the absence of foam lamellae. This result, which is currently used as a basic assumption in models for foams through porous media, has been strengthened recently by Eftekhari & Farajzadeh [6].

It was suggested that the first regime ($r \leq 0.25$) is related to the decrease in the density of bulk pore foam channels to the advantage of surface channels. As the bubble-to-grain further increases, foam microstructure changes dramatically and a new liquid network is activated, where large liquid bridges connected by surface channels replace the liquid network specific to bulk foams. The modelling of these effects is under investigation and will be published in a forthcoming contribution.

| | |
|---|---|
| $D_p$ | diameter of the monodisperse packed beads that forms the porous medium |
| $D_b$ | diameter of the monodisperse bubbles in the foam (inside or outside the porous medium) |
| $r = D_b/D_p$ | size ratio |
| $\phi_p$ | pore volume fraction in the bead packings |
| $\varepsilon_f$ | volume fraction of liquid in the foam |
| $S_w$ | volume fraction of liquid in porous medium. Due to our experimental conditions for the study of the foam-filled samples, we have $S_w \approx \varepsilon_f$ |
| $k_{f0}^{surf}$ | Darcy permeability of the bulk foam, i.e. without any confinement effect, measured by dedicated experiment, for surfactant as mentioned by "surf" = APG or Saponin |

| | |
|---|---|
| $k_f^{surf}$ | Darcy permeability of the foam when confined into the pore space, for surfactant as mentioned by "surf" = APG or Saponin |
| $\tilde{k}_f^{surf} = k_f^{surf}/D_b^2$ | dimensionless foam permeability, for surfactant as mentioned by "surf" = APG or Saponin |
| $k_D$ | Darcy permeability of the foam-filled porous medium |
| $k_D(S_w = 1)$ | Darcy permeability of the liquid-saturated porous medium |
| $k_{rel} = k_D/k_D(S_w = 1)$ | relative permeability of the foam-filled porous medium |

*Table 2: List of the parameters we used.*

## Appendix A: Details about the foam production

The setup we used allows to control liquid foams in terms of bubble size (monodisperse) and liquid volume fraction. Briefly: a flow of nitrogen is pushed to one inlet of a T-junction, while a flow of foaming solution is pushed to the other inlet, producing bubbles at the outlet. The bubbles produced are collected in a vertical glass column. A camera placed at the wall of the column allows to observe them. The control of the liquid outlet (see Fig. 1a) at the bottom of the column permits either to stabilize the position of the foam in the column or to let it exit from the top at a chosen flow rate.

The bubble generator device allows us to change the bubble diameter $D_b$ by tuning the ratio of the nitrogen flow rate $Q_g$ and the solution flow rate $Q_l$. To characterize the generator, *i.e.* to establish the relation $D_b = f(Q_g/Q_l)$, we proceeded as follows: a little of the foam was sucked up with a syringe, to the end of which we then connected a glass capillary (Hirschmann Laborgeräte, Ringcaps 5µL) of diameter 0.29 mm. By drawing some of the foam through the capillary, images were obtained under a microscope which allow direct observation of the confined bubbles (their geometry corresponds to spherocylinders) and deduction of their size. Care was taken to ensure that the bubbles observed were not broken bubbles during their transfer. The relative error on the bubble size is estimated to be within 2 %. Fig. 1b displays the measured $D_b$ values for different liquid/gas flow rate ratios. It is noted that the generator permits to obtain bubbles of 500 µm in diameter at a significant gas flow rate (7 mL/min). Producing efficiently bubbles with diameters smaller than 400 µm or larger than 800 µm requires to change the tee-junction.

In order to impose the liquid fraction of the foam when discharged from the column, it is necessary to control the drainage of the foam during its stay in the column. The simplest way is to impose the output flow rate $Q$, to fix the position of the separation interface between the foam and the liquid in the column (foam height $h$ in Fig. 1a). In practice, maintaining a fixed height of foam in the column consists in evacuating from the bottom of the column the excess liquid introduced with the bubbles from the generator. The liquid volume fraction of the discharged foam was measured by weighting the mass of the liquid contained into a known foam volume. Fig. 1c shows the evolution of the liquid fraction of the discharged foam as a function of the foam height $h$, for $Q = Q_g$ = 10 mL/min. As one can see, this evolution is well-characterized by a power-law function, *i.e.* $\varepsilon_f \approx 0.0026\ h^{-0.90}$, within the range $\varepsilon_f \approx$ 1-8%. Actually, higher liquid fraction could not be achieved by this way. Therefore, in order to vary this parameter over the full range, *i.e.* 1-30%, we add liquid at flow rate $q_a$ directly into the discharged foam, right before the entry in the porous column (see Fig. 1a), where the target liquid fraction can be estimated by volume conservation: $\varepsilon_f \approx (q_a + 0.0026\ Q h^{-0.90})/(q_a + Q)$.

## Appendix B: Details about the measurement of liquid permeability

We present the two methods used to measure the liquid permeability of the reference bulk foams (i.e. unconfined) and the foam-filled porous samples.

*1. Forced drainage*

This measurement method, generally referred to as *forced drainage* [11,12], involves allowing first the foam produced to drain into the column, then pouring surfactant solution down from the top of the column, while measuring the rate at which this excess liquid flows into the foam as a front separating the initial foam, of liquid volume fraction $\varepsilon_{f0}$, from the foam soaked to fraction $\varepsilon_f$. We used this method to characterize both the bulk foam permeability and the foam confined in the porous medium.

Bulk (unconfined) foam: With the 500 µm bubbles produced, it is possible to let the foam drain for about fifteen minutes without observing any ripening, *i.e*. evolution of the bubble size. This step permits to decrease the liquid fraction in the foam in order to better observe the evolution of the liquid front. It is then necessary to know the liquid fraction of the foam after this waiting phase and before pouring the solution. To do this, the drained foam is discharged from the column at a volume flow rate $Q$ and the mass of foam collected in a container for a time $\Delta t$ is weighed. The fraction of liquid contained in this foam is thus: $\varepsilon_{f0} = m/(\rho Q \Delta t)$. Under our experimental conditions we measured $\varepsilon_{f0}$ = 0.5% ±0.2% for APG foam, and $\varepsilon_{f0}$ = 1.8% ±0.2% for saponin foam. It is assumed that these values are unchanged as long as the foam production conditions are unchanged.
After this first phase, the surfactant solution is poured at the top of the column with a so-called imbibition flow rate $q$ (see Fig. B1a), the bottom of the column being completely closed while the top is open to allow the foam expansion. The drainage front is observed with a camera and its passage is detected by light transmission at different positions $z_i$ in the column (see Fig. B1a). For each height $z_i$ a space-time image is obtained, of width $w$ corresponding to that of the image of the column, according to time (or image number $\xi$). We then plot as a function of $\xi$ the gray level $n$ averaged over $w$. These curves clearly show a transition which corresponds to the passage of the front. To determine the speed of the front, we plot the normalized gray level $n^* = (n - n_{min})/(n_{max} - n_{min})$ between 0 and 1 for the different heights $z_i$, as a function of time obtained from image number $\xi$ and the time interval between images in the sequence. This type of figure is shown in Fig. B1b. The passage of the front for each $z_i$ is marked by the value $n^*$ = 0.5, which makes it possible to determine the associated passage times $t_{pi}$. We then plot $z_i - z_1$ as a function of $t_{pi} - t_{p1}$ whose slope directly provides the velocity $v_f$ of the front (see Fig. B1c). From the front velocity data, it is possible to deduce the permeability $k_{f0}$ of the foam. We start by using Darcy's law applied to the gravity flow of the liquid in the foam:

$$\frac{q_i}{S} = \frac{k_{f0}}{\mu}\rho g \quad (B1)$$

In order to compare our results with those of the literature, the permeability is scaled by the square of the bubble size:

$$\tilde{k}_{f0} = \frac{k_{f0}}{D_b^2} = \frac{\mu q_i}{\rho g S D_b^2} \quad (B2)$$

The liquid fraction $\varepsilon$ of the foam behind the front ($\varepsilon_{f0}$ being that before the front passes) is determined by conservation of liquid volume: $v_f(\varepsilon_f - \varepsilon_{f0}) = q_i/S$. Thus, the measurement of $v_f$ provides the liquid fraction:

$$\varepsilon_f = \varepsilon_{f0} + \frac{q_i}{S v_f} \quad (B3)$$

Foam confined in the porous medium: For a few samples, essentially those with large grains (3 and 5 mm) and APG foams, we realized that they were notoriously draining, so we sought to measure their permeability in the same way as for unconfined foams, as described above. For such measurements, the length of the porous column is 160 mm. Foam filling is performed as described in II.C. with a foam containing 5% liquid, and then 10 to 15 min is waited for drainage to decrease the liquid fraction. This fraction, noted $\varepsilon_{f0}$, was measured to be 2.6% ± 0.2%, by comparing the masses of the columns filled with foam and those of the same columns but dry, knowing the volume of grains (their mass and density) initially introduced into the column. For different imposed flow rates, the velocity of the advancing front of the liquid in the medium is measured and processed with the method already presented in previous paragraph. Note however that parameter $S$ has to be replaced by $\phi_p S$ into the previous equations in order to get the permeability of the foam. Similar front passage shapes are obtained as those observed with the foam alone (see Fig. B1), although the presence of the grains decreases the amplitude of the measured intensity signal. These measurements allow us to determine $k_f(\varepsilon_f, D_b, D_g)$, the permeability of the confined foam.

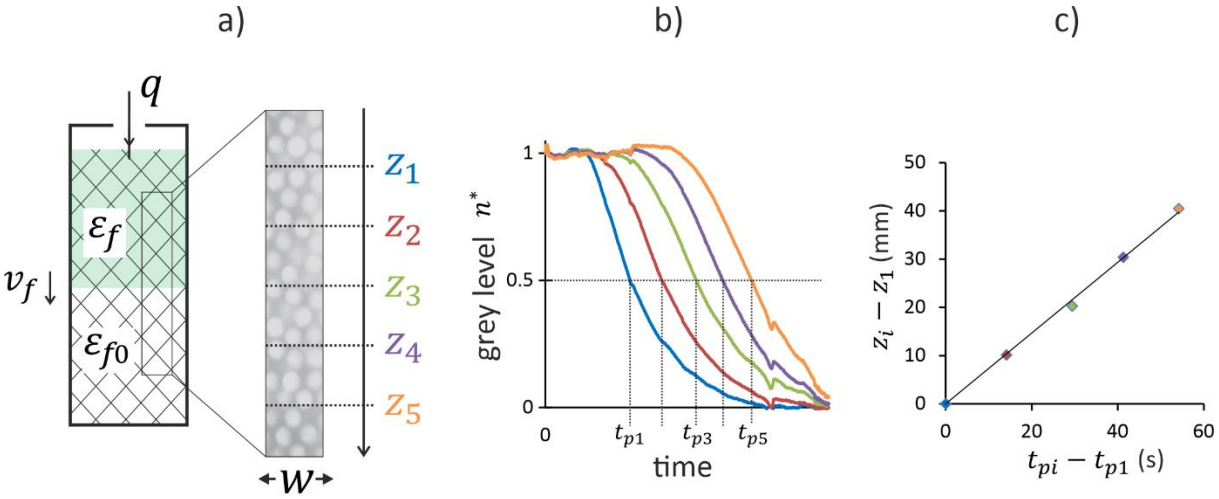


*Figure B1: (a) The position of the drainage front is detected by light transmission at different positions $z_i$ in the column ($\varepsilon_{f0}$ is the initial liquid volume fraction, $\varepsilon_f$ is the value after the passage of the front). (b) To determine the speed of the front, we plot the normalized gray level $n^*$ for the different heights $z_i$, as a function of time. (c) We then plot $z_i - z_1$ as a function of $t_{pi} - t_{p1}$ whose slope directly provides the velocity $v_f$ of the front.*

*2. Falling head permeability test*

For all other samples, we did not observe any appreciable drainage during the 15-20 min during which it can be considered that the ripening has not yet had time to modify the bubble size. We therefore turn to another method described as follows: it consists in imposing a liquid height at the top of the granular/foam column and in following the liquid flow through the column (which is open at the bottom, in contrast to the first method) in the situation where the bubbles are not carried away by the flow. It should be noted that the first method involves the movement of bubbles in the porosity above the drainage front, due to the conservation of volume, and it was used rather for the biggest sizes of grains. The second method requires the capture of bubbles in the porosity of the packing and it was used rather for smaller grain sizes.

To perform our measurements, we reduced the height of the granular column (H = 64 mm) in order to decrease the duration of the experiment. We tested another solution to reduce the time of passage of the liquid through the column, which consisted in increasing the liquid pressure at the head of the column. This proved to be very delicate because bubbles were entrained by the flow so we did not further pursue this way. For the packings studied with this method the bubbles are immobilized by the grains and drainage does not occur or only very little. Therefore, the initial liquid fraction is assimilated to the liquid fraction of the foam used to fill the packing (see paragraph II.C. for more details) and there is no appreciable liquid flow in the absence of any pressure gradient applied to the column. Then a tube is placed above the column, as shown in Fig. B2a, and a volume $V_t$ of surfactant solution is introduced into the tube using a syringe pump. The pressure imposed by the height $z$ of the liquid in the tube allows the liquid to flow into the foam, through the granular packing. The kinetics of this flow is followed by measuring $z$ as a function of time. In this configuration, the liquid flow rate $q$ entering the packing depends on the cross-sectional area $S_t$ of the tube and the variation of height $z$ with time: $q = -S_t\, dz/dt$. Darcy's law allows us to relate the flow rate $q$ of the liquid to the permeability $k_D$ of the medium, i.e. the permeability of the grains + bubbles, assuming that only the liquid is flowing:

$$-\frac{S_t}{S}\frac{dz}{dt} = \frac{k_D}{\eta}\frac{\rho g(z+H)}{H} \quad (B4)$$

The resolution of this equation provides the temporal evolution of the altitude $z$ as a function of the permeability $k_D$:

$$\frac{z+H}{z_0+H} = \exp\left(-\frac{S}{S_t}\frac{k_D}{\eta}\frac{\rho g}{H}t\right) \quad (B5)$$

Preliminary experiments were performed to validate this method, which, to our knowledge, has never been implemented with such foamy system. An example of the results is presented in Fig. B2b for foam with liquid fraction $\varepsilon_f$ = 4% introduced into the packing. Note that the measurement must be carried out over a period not exceeding about 20 minutes in order to limit the possible effects related to foam ripening.

The permeability related to the foam confined into the granular packing can be deduced from the $k_D$ value by the following relation:

$$k_f\left(\varepsilon_f, D_b, D_g\right) = \frac{k_D\left(\varepsilon_f, D_b, D_g\right)}{\phi_p} \quad (B6)$$

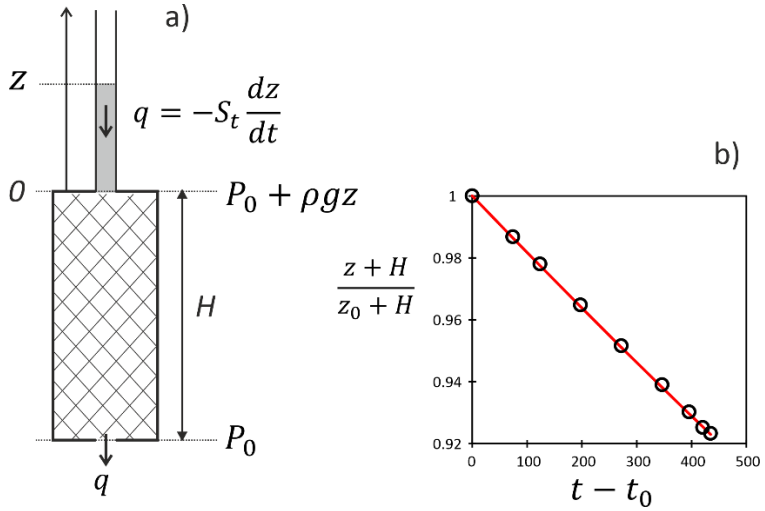

*Figure B2: Darcy method. (a) The liquid height is measured at the top of the granular/foam column which allows the liquid flow through the column to be determined, in the situation where the bubbles are not carried away by the flow. (b) Example of measurement preformed with this method: position of the liquid height as a function of time. Bubble size: 490 µm. Grain size: 2 mm. Liquid volume fraction: 7 vol.%. Permeability value obtained by fitting equation 5: 4.48 $10^{-14}$ $m^2$*

**Acknowledgement**

The authors gratefully acknowledge funding from the Labex MMCD provided by the national program Investments for the Future of the French National Research Agency (ANR-11-LABX-022), and co-funding from the European Space Agency (reference I-2020-02017)

**References**

1. Stevenson, P. *Foam Engineering Fundamentals and Applications*. (John Wiley & Sons, Ltd, 2012).
2. Hirasaki, G. J., Miller, C. A., Szafranski, R., Lawson, J. B. & Akiya, N. Surfactant/Foam Process for Aquifer Remediation. *Proceedings - SPE International Symposium on Oil field Chemistry* 471–480 (1997) doi:10.2118/37257-MS.
3. Rossen, W. R. *Foams in Enhanced Oil Recovery*. *Foams* (Routledge, 1996). doi:10.1201/9780203755709-11.
4. Szymkiewicz, A. *Modelling Water Flow in Unsaturated Porous Media: Accounting for Nonlinear Permeability and Material*. (Springer, 2013). doi:10.1007/978-3-642-23559-7.
5. Bernard, G. G., Holm, L. W. & Jacobs, W. L. Effect of Foam on Trapped Gas Saturation and on Permeability of Porous Media to Water. *Society of Petroleum Engineers Journal* **5**, 295–300 (1965).
6. Eftekhari, A. A. & Farajzadeh, R. Effect of Foam on Liquid Phase Mobility in Porous Media. *Sci Rep* **7**, (2017).
7. Khidas, Y., Haffner, B. & Pitois, O. Capture-induced transition in foamy suspensions. *Soft Matter* **10**, 4137–4141 (2014).
8. Gorlier, F., Khidas, Y. & Pitois, O. Coupled elasticity in soft solid foams. *J Colloid Interface Sci* **501**, 103–111 (2017).
9. Mouquet, A., Khidas, Y., Saison, T., Faou, J.-Y. & Pitois, O. Well-controlled foam-based solid coatings. *Soft Matter* **15**, (2019).
10. Kaddami, A. & Pitois, O. A physical approach towards controlling the microstructure of metakaolin-based geopolymer foams. *Cem Concr Res* **124**, 105807 (2019).
11. Miles, G. D., Shedlovsky, L. & Ross, J. Foam Drainage. *Journal of Physical Chemistry* **49**, 93–107 (1945).

12. Weaire, D., Pittet, N., Hutzler, S. & Pardal, D. Steady-state drainage of an aqueous foam. *Phys Rev Lett* **71**, 2670–2673 (1993).

13. Cantat, I. *et al. Foams: Structure and Dynamics*. (Oxford University Press, 2013).

14. Rouyer, F., Pitois, O., Lorenceau, E. & Louvet, N. Permeability of a bubble assembly: From the very dry to the wet limit. *Physics of Fluids* **22**, 043302 (2010).

15. Carman, P. C. Fluid flow through granular beds. *Transactions, Institution of Chemical Engineers, London* **15**, 150–166 (1937).

16. Kozeny, J. Ueber kapillare Leitung des Wassers im Boden. *Sitzungsber Akad. Wiss.* **136**, 271–306 (1927).